is not derivable from our data. The evaluation of side-chain rotamer populations in both glutamine units reveals that there is a reduced mobility (one rotamer predominating), but there is no fixed side-chain conformation present. The existence of hydrogen bonds can be excluded based on the high-temperature dependence of the exchangeable protons. In summary, all spectroscopic data (that is NMR and circular dichroism) indicate clearly that the pentapeptide exists in a nonrandom, highly organized conformation that is unusual for a peptide of that size.

Acknowledgment. The authors gratefully acknowledge the financial assistance of the Natural Sciences and Engineering Research Council of Canada, the Canadian Medical Research Council, The Central Research Fund of the University of Alberta, and the Alberta Heritage Foundation for Medical Research (through a fellowship to A.O.).

Assignment of Bacteriochlorophyll *a* Ligation State from Absorption and Resonance Raman Spectra

Patricia M. Callahan and Therese M. Cotton*

Contribution from the Department of Chemistry, University of Nebraska—Lincoln, Lincoln, Nebraska 68588-0304. *Received April 6, 1987*

Abstract: Absorption and Soret excitation resonance Raman (RR) spectra have been obtained for a series of coordination forms of monomeric bacteriochlorophyll *a* (BChl *a*). Strong and moderate intensity bands are observed in the RR spectrum at 1609 and 1530 cm^{-1} for five-coordinate species, which shift to 1595 and 1512 cm^{-1}, respectively, in the six-coordinate form. These coordination-sensitive vibrations are independent of the nature of the axial ligand and are suggested to have significant C_aC_m character, while several other less intense coordination-sensitive bands at 1463, 1444, and 1375 cm^{-1} are considered to arise from C_bC_b and C_aN stretching vibrations. These coordination-sensitive RR bands were used to determine BChl *a* ligation state in the solvents used, and structure correlations based on absorption maxima have been developed. The Q_x absorption band position is sensitive not only to BChl *a* Mg^{2+} coordination number but also to the nature of the axial ligand, i.e., oxygen, sulfur, or nitrogen. Q_x maxima are observed at 570, 575–580, and 582 nm for five-coordinate oxygen, sulfur, and nitrogen ligands, respectively, and at 590–595 and 605–612 nm, for six-coordinate oxygen and nitrogen species, respectively. The Q_y absorption maximum is insensitive to coordination number changes but is dependent on the nature of the axial ligand: 770 nm for oxygen ligand(s) and 775 nm for nitrogen ligand(s). A similar series of absorption and Soret excitation RR spectra were obtained for the demetalated form of BChl *a*, BPheo *a*. The Q_x maxima and RR spectra are insensitive to the solvents used, thereby confirming that coordination changes are responsible for the observed BChl *a* spectral shifts. The structure correlations for monomeric BChl *a* established here, based on the absorption and RR data, are discussed with reference to earlier molecular orbital calculations.

The distribution and function of bacteriochlorophyll *a* (BChl *a*) in bacterial photosynthesis range from a water-soluble antenna protein in the green bacterium *Prosthecochlorus aestuarii* to membrane-bound antenna proteins in the purple photosynthetic bacteria, e.g., *Rhodobacter sphaeroides* and *Rhodospirillum rubrum*, and to the reaction center (RC) pigments of green and purple bacteria.[1-3] The structure of BChl *a*, shown in Figure 1, is a tetrahydroporphyrin with a condensed Vth ring and with conjugated ketone functionalities at position 2 (acetyl) and position 9 (ketyl). The coordination sphere of Mg^{2+} is not satisfied by the four pyrrole nitrogens, and a fifth ligand is always present, either as an exogenous ligand in monomeric systems or as the C_2 acetyl or C_9 ketyl groups of a neighboring BChl *a* molecule in self-aggregates. In these cases the central Mg^{2+} remains out of the plane of the pyrrole nitrogens. A sixth ligand, of sufficient base strength, can be added to the coordination sphere which forces the central metal down into the plane of the bacteriochlorin ring.

The absorption spectrum of BChl *a* is characterized by an intense Soret band in the near-UV composed of B_x and B_y components, a band of moderate intensity in the visible region, Q_x, and another intense band in the near-infrared region of the spectrum, identified as Q_y. Both of the Q bands have vibrational overtones at approximately 1300 cm^{-1} to higher energy of the 0–0 electronic transitions. Several molecular orbital calculations of the porphyrins and (bacterio)chlorins have been carried out[4-7] and their electronic energy levels can be described by using the four-orbital model of Gouterman.[8,9] The Q_y and Q_x transition dipoles are oriented along the unsaturated rings I and III and the reduced rings II and IV,[10,11] respectively, as shown in Figure 1.

In its different protein environments the Q_y band of BChl *a* has been observed to range from 800 to 917 nm as a result of environment and exciton effects.[12,13] However, an exact description of very few systems has been made at this time. In recent calculations of the reaction center pigments of *Rh. viridis* and *Rb. sphaeroides* an ad hoc red shift of the Q_y band of monomeric BChl *a* from 770 to 807 nm for accessory BChl *a* and to 837 nm for the "special pair" P870 was needed in order to fit the exciton calculations to the known crystal structure coordinates of the pigments.[14] In this paper we are concerned with the spectral shifts

(1) Thornber, J. P.; Trosper, T. L.; Strouse, C. E. In *Photosynthetic Bacteria*; Clayton, R. K., Sistrom, W. R., Eds.; Plenum: New York, 1978; pp 133–160.
(2) Wraight, C. A. In *Photosynthesis: Energy Conversion by Plants and* Bacteria; Govindjee, Ed.; Academic: New York, 1982; Vol. 1, pp 19–61.
(3) Okamura, M. Y.; Feher, G.; Nelson, N. In *Photosynthesis: Energy Conversion by Plants and Bacteria*; Govindjee, Ed.; Academic: New York, 1982; Vol. 1, pp 197–272.
(4) Seely, G. R. *J. Chem. Phys.* **1957**, *27*, 125–133.
(5) Weiss, C. Jr. *J. Mol. Spectrosc.* **1972**, *44*, 37–80.
(6) Petke, J. D.; Maggiora, G. M.; Shipman, L.; Christofferson, R. E. *Photochem. Photobiol.* **1979**, *30*, 203–223.
(7) Petke, J. D.; Maggiora, G. M.; Shipman, L. L.; Christofferson, R. E. *Photochem. Photobiol.* **1980**, *32*, 399–414.
(8) Gouterman, M. *J. Chem. Phys.* **1959**, *30*, 1139–1161.
(9) Gouterman, M. *J. Mol. Spectrosc.* **1961**, *6*, 138–163.
(10) Goedheer, J. C. In *The Chlorophylls*; Vernon, L. P., Seely, G. R., Eds.; Academic: New York, 1966; pp 147–184.
(11) Moog, R. S.; Kuki, A.; Fayer, M. D.; Boxer, S. G. *Biochemistry* **1984**, *23*, 1564–1571.
(12) Pearlstein, R. In *Photosynthesis: Energy Conversion by Plants and Bacteria*; Govindjee, Ed.; Academic: New York, 1982; Vol. 1, pp 293–330.
(13) Garcia, D.; Parot, P.; Vermeglio, A.; Madigan, M. T. *Biochim. Biophys. Acta* **1986**, *850*, 390–395.

0002-7863/87/1509-7001$01.50/0

Table I. Absorption Maxima (nm) and RR Band A Frequencies (cm^{-1}) for BChl *a* Including Solvent Properties[a]

ligand	B_y	B_x	Q_x	Q_y	DN	ϵ	band A
1. CH_2Cl_2	355	390	580	774	0	9.1	1609
2. C_6H_6	360	395	580	780	0.1	2.3	1609
3. acetone	355	390	574	768	17.0	20.7	1609
4. ethyl ether	355	390	570	770	19.2	4.3	1609
5. EtSH	356	390	576	773			1609
6. THT	362	394	580	776			1609
7. 0.5 M 2-MeIm (CH_2Cl_2)	360	390	582	775			1609
8. 100 mM py (CH_2Cl_2)	360	390	582	776	33.1	12.3	1609
9. DMF	360	(390)[c]	582/600[b]	772	26.6	36.7	1609/1595[b]
10. DMSO	365	(390)	586/598	773	29.8	46.7	1609/1595
11. EtOH	360		(580)/595	770	31.5	24.3	(1609)[c]/1595
12. MeOH	360		595	768	25.7	32.7	1595
13. THF	365	392	594	770	20.0	7.6	1595
14. pyridine	373		610	776	33.1	12.3	1595
15. *N*-MeIm	363	390	618	778			1595

[a] Abbreviations: EtSH, ethanethiol; THT, tetrahydrothiophene; 2-MeIm, 2-methylimidazole; DMSO, dimethyl sulfoxide; THF, tetrahydrofuran; *N*-MeIm, *N*-methylimidazole; DN, donor number; ϵ, dielectric constant. [b] Two values indicate mixed coordination and two peaks present in the spectrum. [c] Peak positions in parentheses indicate poorly resolved shoulders.

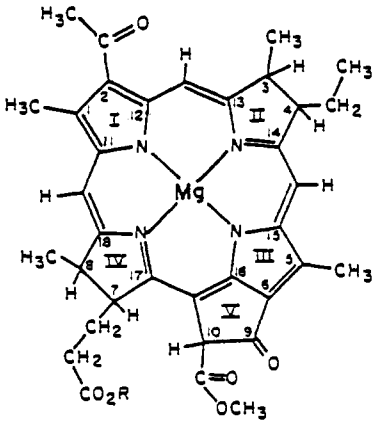

Figure 1. Structure of BChl *a*.

of monomeric BChl *a* as a function of known structural changes. With this approach a more complete description of the structure and environment of BChl *a* in vivo can be made.

The red shift of the Q_x band of BChl *a* in polar solvents was noted by Weigl[15] and later suggested to have a structural basis by Evans and Katz.[16] The latter observed that the Q_x band position of BChl *a* occurred at 580 nm for five-coordinate Mg^{2+} and at 610 nm for six-coordinate Mg^{2+} with pyridine (py) as axial ligand. Cotton and Van Duyne[17] further substantiated this conclusion by obtaining resonance Raman (RR) spectra of BChl *a* as a function of pyridine concentration. Distinct spectra were observed for each coordination geometry with 457.9-nm excitation. By using Soret region laser excitation we are able to lower the detection limits of BChl *a* RR scattering from the millimolar to the micromolar concentration range, and we have observed similar coordination-sensitive marker bands throughout the Soret region (350–450 nm). These RR coordination marker bands are found to be independent of the nature of the axial ligand whereas the Q_x band position is dependent on the Lewis base strength of the added ligand. Since base strength usually increases along the series oxygen, sulfur, and nitrogen, discrete Q_x band positions are seen for each of these ligand structures. The position of the Q_y band is fairly insensitive to changes in axial coordination but reflects changes at the ring peripheral substituents. These absorption shifts are consistent with the molecular orbital calculations of Petke et al.[7] With these new correlations it is possible to identify the number and nature of the axial ligands of monomeric BChl *a* from the combined information provided by absorption and RR spectroscopies.

Experimental Section

The BChl *a* used in these studies was purified by chromatography on powdered sucrose according to published procedures.[18] Bacteriopheophytin *a* (BPheo *a*) was prepared by acidification of BChl *a* followed by chromatography on powdered sucrose. Both pigments were dried by codistillation from CH_2Cl_2. Solvents were purchased from Burdick and Jackson (distilled in glass) or were of the highest grade available. Pyridine and THF were further purified by chromatography on activated alumina (Woelm Grade I, basic) and vacuum-distilled from CaH_2. All other solvents were used as received without further purification. Samples for resonance Raman spectroscopy were placed in 5-mm Pyrex tubes, vacuum degassed by using three freeze–pump–thaw cycles, and sealed under vacuum. Absorption specra were taken in a 1-mm-path length cuvette before and after the Raman experiment to monitor sample integrity.

The laser excitation sources were Coherent Ar^+ (Innova 90-5) and Kr^+ (Innova 100) lasers. Typical laser powers at the sample were 5 mW, and backscattering geometry was used for sample irradiation. The Raman instrumentation consisted of a Spex Triplemate 1877 and intensified diode array detector (PARC 1420) coupled to a multichannel analyzer (PARC OMA II) which was used to accumulate and process the data. An 1800 groove/mm grating was used in the spectrograph stage, and indene was used for frequency calibration. Electronic absorption spectra were recorded on a Cary 14 spectrometer equipped with a Hamamatsu R928 red-sensitive photomultiplier tube.

Results

Absorption Spectral Effects. Representative absorption spectra of BChl *a* as a function of the nature of axial ligand are shown in Figure 2. The Q_x band shifts from 575 to 610 nm along the following series of solvents: acetone, 2-methylimidazole (2-MeIm) in CH_2Cl_2, THF, and py. The Q_y band is fairly insensitive to coordinating solvent, with all the oxygen complexes occurring at $\approx$770 nm and all the nitrogen complexes occurring at $\geq$775 nm. This 5-nm (100-cm^{-1}) shift is small relative to the 50-nm range (1400 cm^{-1}) of the Q_x band. The third type of band shift observed in Figure 2 is the red shift of the Soret maximum from 355 to 373 nm. Evans and Katz[16] had previously pointed out the position of Q_x for five- and six-coordinate BChl *a*–nitrogen complexes, and this figure suggests a similar correlation for BChl *a*–oxygen complexes.

The absorption maxima of several other axial ligation complexes are given in Table I along with solvent dielectric constant and donor number. From the data in Table I, it can be seen that the dielectric constant of the solvent is not a good indicator of the absorption band position. Because of the delocalized π-system of BChl *a* a large change in dielectric constant would not be expected to shift the absorption maximum significantly (i.e., no

(14) Vasmel, H.; Amesz, J.; Hoff, A. J. *Biochim. Biophys. Acta* **1986**, *852*, 159–168.
(15) Weigl, J. W. *J. Am. Chem. Soc.* **1953**, *75*, 999–1000.
(16) Evans, T. A.; Katz, J. J. *Biochim. Biophys. Acta* **1975**, *396*, 414–426.
(17) Cotton, T. M.; Van Duyne, R. P. *J. Am. Chem. Soc.* **1981**, *103*, 6020–6026.
(18) Strain, H. H.; Svec, W. A. In *The Chlorophylls*; Vernon, L. P., Seely, G. R., Eds.; Academic: New York, 1966; pp 21–66.

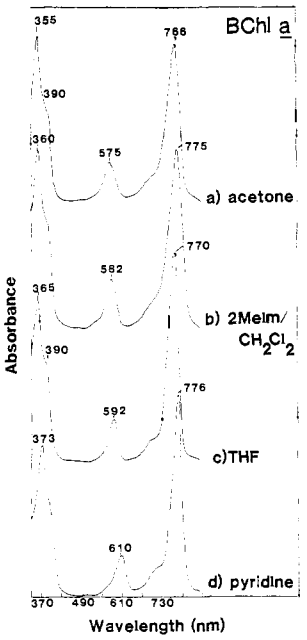

Figure 2. Absorption spectra of BChl *a* in (a) acetone, (b) 0.5 M 2-MeIm and CH_2Cl_2, (c) THF, and (d) pyridine. Concentration of BChl *a* is approximately 100 μM for all samples; path length = 1 mm.

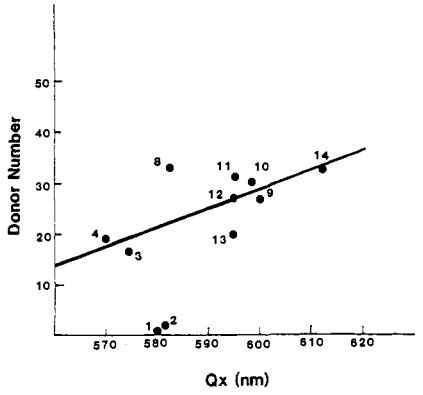

Figure 3. Plot of Q_x absorption maxima versus donor number for the samples listed in Table I. In cases where mixed coordination is observed, the data for the predominant species is plotted.

large change in dipole moment is expected on excitation from the ground to excited state). In the absence of BChl *a*–ligand equilibrium constants, there are several empirical parameters that can be used to quantitate ligand σ-bond strengths,[19] solvent polarity,[20] and complexation ability.[21] Since the Gutmann donor number scale[20,21] has been used successfully as a measure of solvent coordinating ability in iron porphyrins,[22] this parameter is listed with the solvent data in Table I. The Q_x band position does approximately follow the Gutmann donor number[21] of the solvent (Figure 3). The general trend is as follows: the greater the donor number, the larger the red shift observed for Q_x. Two points that lie furthest off the curve in Figure 3 are points 1 and 2, CH_2Cl_2 and C_6H_6, respectively. These low donor number solvents are noncoordinating solvents in which BChl *a* is known to be aggregated.[23,24] In the earlier work of Evans and Katz a distinction between coordinating and noncoordinating solvents was not made in the correlations of absorption maxima with coordination

(19) Drago, R. S.; Kroeger, M. K.; Stahlbush, J. R. *Inorg. Chem.* **1981**, *20*, 306–308.
(20) Reichardt, C. In *Solvent Effects in Organic Chemistry*; Ebel, H. F., Ed.; Verlag Chemie: New York, 1979; Vol. 3.
(21) Gutmann, V. In *Donor–Acceptor Approach to Molecular Interactions*; Plenum: New York, 1978; p 20.
(22) Bottomley, L. A.; Kadish, K. M. *Inorg. Chem.* **1981**, *20*, 1348–1357.
(23) Ballschmiter, K.; Truesdell, K.; Katz, J. J. *Biochim. Biophys. Acta* **1969**, *184*, 604–613.
(24) Heald, R. L.; Cotton, T. M. *J. Phys. Chem.* **1987**, *91*, 3891–3898.

Table II. Absorption Maxima (nm) of BPheo *a* Plus Donor Number and Dielectric Constant for Several Solvents

ligand	Soret	Q_x	Q_y	DN	ϵ
CH_3CN	360, 384	523	744	14.1	38.8
acetone	355, 380	523	740	17.0	20.7
ethyl ether	355, 385	523	748	19.2	4.3
THF	356, 384	525	747	20	7.6
DMSO	355, 380	526	750	29.8	46.7
EtOH	356, 385	527	748	31.5	24.3
pyridine	360, 388	529	753	33.1	12.3

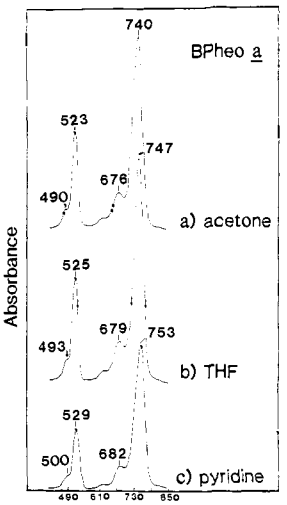

Figure 4. Absorption spectra of BPheo *a* in (a) acetone, (b) THF, and (c) pyridine. Concentration of BPheo *a* is approximately 100 μM; cuvette path length = 1 mm.

number.[16] From the data of Figure 3, however, it is apparent that the spectra of aggregated BChl *a* do not follow the same pattern as monomeric BChl *a*.

Another data point in Figure 3 that falls slightly off the curve is point 8, five-coordinate BChl *a* in CH_2Cl_2 plus 0.1 M pyridine. The point for neat pyridine (point 14) does lie close to the least-squares fit line, which indicates that the donor number scale is a better predictor of Q_x band position in neat solvents than in mixtures.

To establish further the link between BChl *a* coordination state and Q_x absorption maximum, the absorption spectra of demetalated BChl *a*, BPheo *a*, were obtained for the same series of solvents (Figure 4 and Table II). Since no coordination change or self-aggregation is possible for BPheo *a* in these solvents, the shifts observed should reflect only changes in dielectric constant or peripheral substituent effects. In Figure 4, the complete range of Q_x band positions observed is 523 nm in acetone to 529 nm in py. This 6-nm (220-cm^{-1}) shift is very small compared to the 50-nm shift observed for the Q_x band of BChl *a*. Similar to that observed for BChl *a*, the Q_x band position of BPheo *a* in Table II does not follow the solvent dielectric constant but rather increases slightly as the solvent donor number increases. Conversely, the Q_y band position of BPheo *a* is more sensitive to solvent than that of BChl *a*. Its position varies from 740 nm in acetone to 753 nm in py (Δ = 220 cm^{-1}) and increases with the donor number of the solvent also. The large shift in the Q_x band position of BChl *a* seems to indicate that it is a valid indicator of coordination state for both oxygen- and nitrogen-containing axial ligands. This correlation will be established more firmly in the next section where structural marker bands in the Soret excitation RR spectra of BChl *a* are presented.

Resonance Raman Spectral Effects. RR spectra of BChl *a* provide information about the bacteriochlorin ring vibrations and the conjugated ketone groups at positions 2 and 9. Two bands in the 300-cm^{-1} region of the Soret excitation RR spectrum of BChl *a* have been identified as coordination sensitive by isotopic substitution studies.[25] Such low-frequency spectra were not

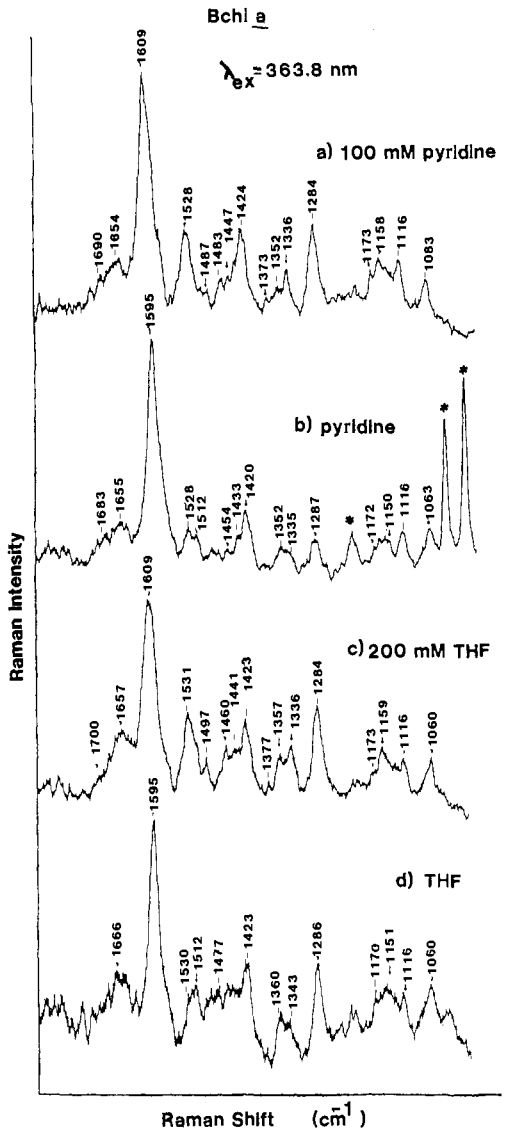

Figure 5. Resonance Raman spectra of BChl *a* in CH_2Cl_2 with 363.8-nm excitation: (a) 100 mM pyridine; (b) neat pyridine; (c) 200 mM THF; (d) neat THF. BChl *a* concentration was approximately 100 μM for all samples. Laser power, 5 mW; spectral resolution, 6 cm^{-1}. Solvent and ligand bands are marked with asterisks.

obtained in the present study, however, owing to overlapping solvent bands. Another study utilized 457.9-nm excitation, preresonant with the B state; because of the smaller preresonant enhancement, concentrations of BChl *a* of 10 mM were required.[17] With Soret region RR spectroscopy concentrations of 100 μM BChl *a* can be studied, thus extending the concentration range of pigment that can be used for structure elucidation.

Cotton and Van Duyne identified two major high-frequency RR vibrational band shifts in a titration of BChl *a* with pyridine.[17] As the central Mg^{2+} changed from five- to six-coordinate, a shift of the 1609-cm^{-1} band to 1595 cm^{-1} (designated band A) and a splitting of the 1529-cm^{-1} band into two bands at 1530 and 1519 cm^{-1} (band B) was observed. These data were obtained with 457.9-nm excitation and the authors concluded that this resulted in a preresonant Raman spectrum with the nearby intense Soret band at ≈360 nm. This conclusion is borne out by the observation of similar vibrational shifts of Soret excitation (363.8 nm) RR spectra occurring with a pyridine titration of BChl *a* in CH_2Cl_2 (Figure 5a, and b). As the concentration of pyridine increases, the RR spectrum of BChl *a* in CH_2Cl_2 displays the following major shifts: the 1609-cm^{-1} band (band A) observed at 100 mM pyridine

(25) Lutz, M. In *Advances in Infrared and Raman Specroscopy*; Clark, R. J. H., Hester, R. E., Eds.; Wiley: New York, 1983; Vol. 11; pp 211–300.

Table III. Comparison of Soret Excitation Resonance Raman Spectra of Five- and Six-Coordinate BChl *a* Species (cm^{-1})

five-coordinate	six-coordinate	assignment
1609	1595	$\nu(C_aC_m)$
1528	1528	$\nu(C_aC_b)$
	1512	$\nu(C_aC_m)$
1463	1445	$\nu(C_bC_b)$, $\nu(C_aC_m)$
1444	1433	$\nu(C_bC_b)$, $\nu(C_aC_m)$
1375	1361	$\nu(C_aN)$
1335	decrease intensity	$\nu(C_aN)$
1285	1285	$\delta(C_mH)$
1116	1116	$\delta(C_mH)$
1060	1060	$\delta(C_mH)$

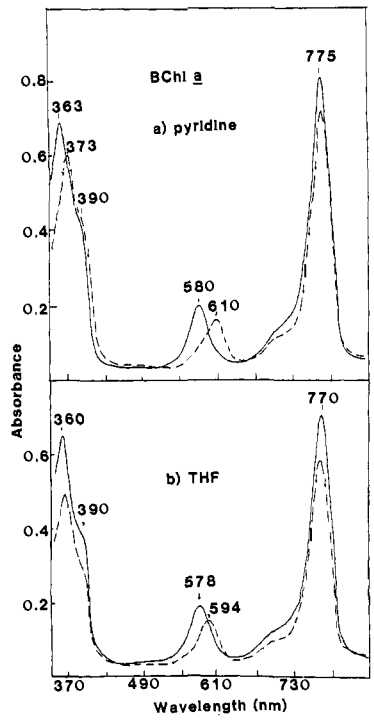

Figure 6. Absorption spectra of BChl *a* in CH_2Cl_2: (a) (—) 100 mM pyridine, (- - -) 2 M pyridine; and (b) (—) 200 mM THF, (- - -) 4 M THF.

shifts to 1595 cm^{-1} at 2–12 M pyridine and the 1528-cm^{-1} band (band B) decreases in intensity and develops a shoulder at 1512 cm^{-1}. The minor band shifts observed are 1463 to 1455 cm^{-1} and 1445 to 1435 cm^{-1}, and decreases in intensity occur at 1375 and 1335 cm^{-1}. Several bands remain constant throughout the titration at 1285, 1116, and 1060 cm^{-1}. The band shifts are summarized in Table III.

Similar spectra are obtained throughout the Soret region (data not shown) and the largest enhancement of the BChl *a* conjugated ketone functional groups, C_2 acetyl and C_9 ketyl, observed in the range 1640–1705 cm^{-1}, is obtained with 363.8-nm excitation. The C_2 and C_9 (C=O) vibrations remain broad and poorly resolved at 1650–1670 and 1680–1700 cm^{-1}, respectively, throughout the titration. The absorption spectra of the samples in Figure 5a,b are reproduced in Figure 6a. From these two figures it can be seen that, for the sample containing 100 mM pyridine, the Q_x band position of 582 nm correlates with a RR band A position of 1609 cm^{-1} and at 2 M pyridine, Q_x occurs at 610 nm with a band A frequency of 1595 cm^{-1}.

To ensure that the RR band shifts observed in Figure 5a,b are sensitive to BChl *a* coordination number and independent of the chemical nature of the axial ligand, RR and absorption spectra of BChl *a* plus THF are shown in Figure 5c,d. At 200 mM THF, the band A position is 1609 cm^{-1} and shifts to 1595 cm^{-1} in neat THF (12.3 M). Band B splits into two peaks at 1528 and 1512 cm^{-1} in Figure 5d, and the smaller band shifts in the 1400-cm^{-1} region are not as clear although intensity decreases at 1374 and 1330 cm^{-1} are observed. The characteristic five-coordinate BChl

Table IV. Structural Correlations of Monomeric BChl *a* in Coordinating Solvents

	Q_x, nm	Q_y, nm	RR band A, cm^{-1}
5-coord oxygen	570–575	770	1609
(hydrogen bond, aq)[a]	(580–585)	(773)	(1609)
5-coord sulfur	575–580	773–776	1609
5-cord nitrogen	583	775	1609
(hydrogen bond, phenol)[b]	(595)	(785)	
6-coord oxygen	590–595	770	1595
(hydrogen bond, phenol)[c]	(600)	(790)	
6-coord nitrogen	610–618	775–778	1595

[a] BChl *a* in 3% TX-100, 100 mM potassium phosphate, pH 7.4. [b] BChl *a* in CH_2Cl_2 plus 0.5 M 2-MeIm and 3 M phenol. [c] BChl *a* in CH_2Cl_2 with 5 M phenol.

a RR spectrum with an oxygen donor fifth ligand corresponds to a Q_x position of 575 nm and the six-coordinate oxygen ligand species to a 594 nm Q_x band maximum.

Because the free-base form of BChl *a*, BPheo *a*, is unable to undergo changes in coordination, inspection of its RR spectrum in a variety of solvents demonstrates the sensitivity of the bacteriochlorin ring vibrations to dielectric properties of the solvent. The spectra of all the solvents listed in Table II are identical within experimental error (data not shown) and they are similar, except for small intensity differences, to the previously published spectrum of BPheo *a* in CH_2Cl_2.[17] In the absence of a possible coordination change, there are no vibrational band shifts for BPheo *a* as a function of solvent. Therefore, we can conclude that the vibrational band shifts observed for BChl *a*, as enumerated above, are a good indicator of central metal coordination geometry and that the BChl *a* RR spectra are independent of the nature of axial ligand (oxygen vs nitrogen) for a given coordination geometry.

By using these RR band correlations for the solvents listed in Table I, one can establish Mg^{2+} coordination number, and trends in the absorption band position can be identified. The band A frequency position of BChl *a* in all the solvents studied is given in the last column in Table I. Table IV reorganizes the data from Table I by making use of the structural conclusions available from the RR data and lists the observed values of Q_x and Q_y absorption bands for the different types of axial ligand complexes studied. The data are plotted in Figure 7 for a more graphic representation of the information. It is seen that the Q_x band maximum of each of the following categories falls into separate wavelength regions: five-coordinate, oxygen, sulfur, and nitrogen; six-coordinate, oxygen and nitrogen. This ordering of ligand complexes also follows approximately the Lewis base strength of the donor molecules. The Q_y band position varies over a much smaller range and is more sensitive to the nature of the ligand (oxygen vs nitrogen) than coordination number.

Also included in Table IV and Figure 7 are absorption maxima of several hydrogen-bonded BChl *a* systems.[26] Hydrogen bonding shifts both Q_x and Q_y absorption maxima to the red: 10–15 nm for Q_x and 5–20 nm for Q_y. Phenol was used as hydrogen donor in two of the examples because of its previously demonstrated strong hydrogen-bonding ability to the peripheral aldehyde substituent of heme *a*.[27] Although this is not an exhaustive hydrogen bond study, the two systems should give some indication of the range of absorption shifts possible from hydrogen bonding. In these examples (Figure 7 and Table IV) the additional hydrogen bond shift in Q_x (≈10 nm) is fairly consistent for each ligation species studied, whereas the position of Q_y displays an increasing red shift through the series five-coordinate oxygen, five-coordinate nitrogen, and six-coordinate oxygen. The large Q_y red shift (20 nm) manifest in the six-coordinate oxygen example may be a result of a greater ring planarity and therefore greater overlap of C_2 and C_9 ketone groups with the bacteriochlorin π-system. Hydrogen-bonding effects on the absorption spectrum of BChl *a* shift

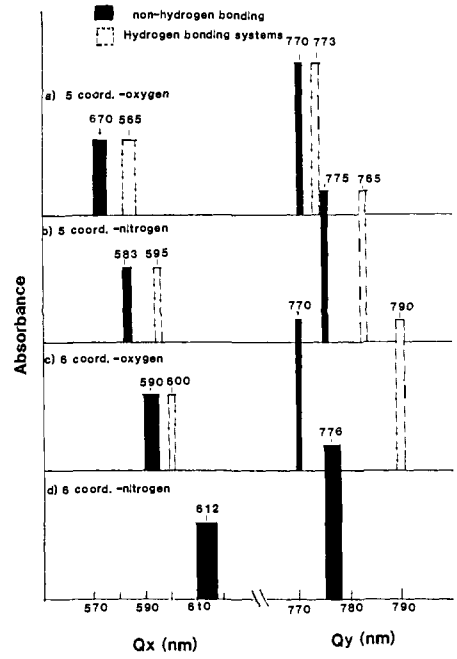

Figure 7. Histogram of absorption spectra of monomeric BChl *a* in hydrogen-bonding and non-hydrogen-bonding solvents as a function of coordination and ligand. Bandwidths indicate the range of wavelength maxima observed; intensities are not meant to reflect true relative intensities.

the coordination-sensitive Q_x band and make it difficult to identify the coordination number of an unknown BChl *a* sample by inspection of the absorption spectrum alone. Therefore, the Soret region RR spectrum is needed for an exact description of the BChl *a* structure. The position of the coordination marker bands, bands A and B, identifies the coordination state, and the position of the C_2 and C_9 (C=O) stretching frequencies identifies the presence of hydrogen bonding; depending on the strength of the hydrogen bond, ν(C=O) can be shifted to lower frequency by 10–40 cm^{-1}.[25] Thus, a complete structural description of monomeric BChl *a* can be made by inspection of its absorption and Soret region RR spectrum.

Discussion

BChl *a* Electronic Transitions. In metalloporphyrin and metallochlorin absorption spectra, the electronic transitions are best understood in terms of the four-orbital model of Gouterman;[8,9] the transitions between two nearly degenerate HOMOs and two LUMOs interact and mix to give an intense Soret band and weak absorption in the visible region. Because of the opposed reduced rings II and IV of the bacteriochlorin macrocycle, a condensed Vth ring, and conjugated carbonyl groups at C_2 and C_9, the molecular axes, *x* and *y*, of BChl *a* are distinct, and the visible and near-IR absorption properties can be approximated as separate transitions from two low-lying molecular obitals. These are designated 1–1* for Q_y and 2–1* for Q_x (Figure 8), in the terminology of Petke et al.[7] The oribtal labels 1, 2, 1*, and 2* of BChl *a* are related to the a_{1u} (b_2), a_{2u} (b_1), e_g (c_2), and e_g (c_1) orbital notation, respectively, of Gouterman for the porphyrin systems.[9] The Q_x transition also contains significant 1–2* character (~40%),[7] which is similar to the metalloporphyrin Q_{0-0} transitions. These mixed transitions result in a weakly absorbing visible band and intense Soret band for Q_x in BChl *a*. The Q_y transition, on the other hand, is composed almost entirely of the 1–1* orbital description,[7] which therefore results in two equally intense bands in the visible (or near-IR) and Soret region, as is observed.

The ground-state MO 2 has electron density at all four pyrrole nitrogens and the methine carbons, while MO 1 has no electron density at the nitrogen or methine positions but rather the electron density is located at the α- and β-carbon positions. Both excited states, 1* and 2*, have electron density on two nitrogen atoms,

(26) The MeOH and EtOH data of Table I constitute only weakly hydrogen-bonded systems, so these data are included in the non-hydrogen-bonding solvents category.

(27) Babcock, G. T.; Callahan, P. M. *Biochemistry* **1983**, *22*, 2314–2319.

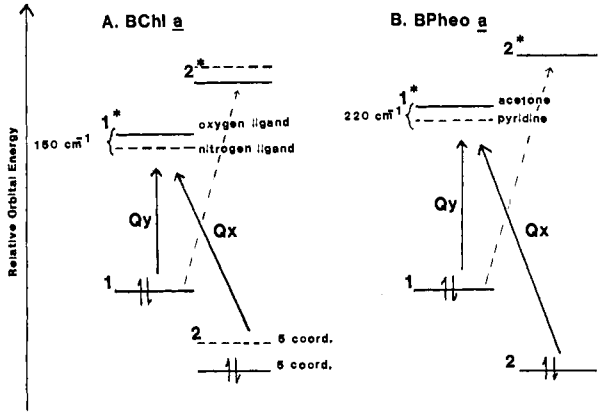

Figure 8. The Q_y and Q_x transitions are labeled as (1–1*) and (2–1* and 1–2*), respectively. (A) For BChl *a* the experimental spectral shift induced by coordination change is indicated by a raising of MO 2. Within a coordination state, a change of ligand must affect the excited-state MO 1* and MO 2* orbitals. (B) For BPheo *a* the observed spectral shifts upon changing solvent are indicated as a lowering of the MO 1* energy level. See text for further details.

but the methine and α-carbon positions differ by a 90° rotation in their electronic distribution around the dihydrophorbin ring. By using these molecular orbital descriptions the empirical correlations presented above for the absorption spectra of BChl *a* as a function of ligation state can be understood from a theoretical perspective.

The gross structural change accompanying an increase from five- to six-coordinate Mg^{2+} results in the out-of-plane central metal being forced down into the plane of the ring concomitant with core expansion. In this six-coordinate, in-plane Mg^{2+} structure, the central metal interacts more strongly with the pyrrole nitrogens, thus raising the energy of the ground-state orbital MO 2 (Figure 8). In metalloporphyrins, the MO 2 orbital (a_{2u}) is also raised in energy upon change from five- to six-coordinate[28] and it is sensitive to the electronegativity of the central metal.[8,29] The effect on the excited states 1* and 2* of BChl *a* is smaller because there is electron density on only two of the pyrrole nitrogen atoms. The net result is a 750–800-cm^{-1} red shift of the Q_x transition in changing from five- to six-coordinate Mg^{2+}.

The insensitivity of the Q_y band position to change in coordination structure can be explained by reference to the molecular orbital calculations of Petke et al.[7] The constancy of Q_y absorption maximum for both oxygen ligation species at 770 nm and for both nitrogen species at 775 nm suggests that coordination changes alone have no effect on the energy of the 1–1* (Q_y) electronic transition. Since the ground-state RR vibrations remain constant within a given coordination state for different axial ligands, this implies that the absorption red shift must arise from changes in the excited-state energy levels. As noted above, the ground-state MO 1 has no electron density on the pyrrole nitrogens, so the only energy levels that can be affected by the nature of the axial ligand (O, S, or N) are the excited-state MO 1* and MO 2*. The absorption and RR results are consistent with a lowering in energy of MO 1*.

The gradual red shift of Q_x within a given coordination state as the nature of the axial ligand is changed must also be caused by changes in excited-state energy levels. The Q_x transition contains contributions from both 2–1* and 1–2* configurations so a shift in one or both of these energy levels could effect a red shift of Q_x. This red shift correlates with the donor ability of the solvent; for example, Q_x shifts from 594 nm for bis-oxygen to 610 nm for bis-nitrogen ligation. With the exception of sterically hindered ligands (e.g., 2-MeIm) the Gutmann donor number is a useful predictor of BChl *a* coordination geometry and also of Q_x band position.

A shift in excited-state energy levels can also explain the shifts observed in the BPheo *a* absorption spectra (Figure 4 and Table II). The molecular orbital descriptions and transitions are very similar for BPheo *a* and BChl *a*,[7] and the small shifts in Q_x and Q_y of 5–10 nm also follow the donor number ordering of the solvents. Since the RR spectra do not change for BPheo *a* in the range of solvents presented here, the absorption shifts must arise from a lowering of the electronic excited-state energy level MO 1* (Figure 8B). On an energy scale, both Q_x and Q_y are shifted by 220–250 cm^{-1} on changing the solvent from acetone to pyridine. The molecular orbital calculations[7] also explain the more dramatic effects of hydrogen bonding on the Q_y vs Q_x absorption maxima. There is a change in electron density at both C_2 and C_9, acetyl and ketyl functional groups for the 1–1* (Q_y) transition whereas no change in electron density for these groups is calculated for 2–1* (Q_x).

This spectral correlation with coordination geometry has not been observed for heme or chlorophyll molecules because the *x*- and *y*-polarized transitions are close in energy and the visible and Soret transitions mix. A weak coordination-sensitive band has been observed for Chl *a* at 633 nm[16,30] but the distinct pattern of coordination and absorption spectra observed here is dependent on the large separation in energy of the *x* and *y*-polarized transitions as a result of the reduced pyrrole rings I and III. Similar correlations between the Soret maxima with ligand and coordination geometry are difficult because of the multiple configurations responsible for light absorption in the near-UV region.[7]

Resonance Raman Spectra. Over the past 10 years, an inverse correlation between the center-to-nitrogen distance (or porphyrin core size) and frequency position has been established for the high-frequency vibrations of metalloporphyrin RR spectra.[31–34] Similar trends have been observed recently for metallochlorins and chlorophyll species.[35–38] Very few RR studies have been done on BChl *a* model compounds although several BChl–protein systems have been studied by Lutz and co-workers.[39–41] With reference to the normal coordinate analysis of Abe et al.,[42] the metalloporphyrin vibrations that display the greatest sensitivity to core size are those bands with the largest C_aC_m stretching character, i.e., those vibrations that are most sensitive to the electron density on the methine carbon atoms. Other high-frequency vibrations which are also sensitive to core size are C_bC_b stretching vibrations. These bands are more difficult to interpret because in some cases they are also sensitive to peripheral substituent effects.[43]

As discussed above, the structural change that occurs as the BChl *a* coordination number increases is the core expansion as Mg^{2+} is forced into the plane of the ring. The major RR band shifts observed in this process are frequency decreases from 1609 to 1595 cm^{-1} (band A) and 1528 to 1512 cm^{-1} (band B). This is indicative of a large amount of C_aC_m stretching character in these vibrations as previously suggested.[17,25] The other observed band shifts most likely arise from mixed vibrations with C_bC_b, C_aC_m, and C_aN stretching characteristics (Table III). The vibrations that remain constant for the two coordination states

(28) Gouterman, M. In *The Porphyrins*; Dolphin, D., Ed.; Academic: New York, 1978; Vol. III, pp 1–165.
(29) Shelnutt, J. A.; Ondrias, M. R. *Inorg. Chem.* **1984**, *23*, 1175–1177.
(30) Renge, I.; Avarmaa, R. *Photochem. Photobiol.* **1985**, *42*, 253–260.
(31) Spaulding, L. D.; Chang, C. C.; Yu, N.-T.; Felton, R. H. *J. Am. Chem. Soc.* **1975**, *97*, 2517–2525.
(32) Felton, R. H.; Yu, N.-T. In *The Porphyrins*; Dolphin, D., Ed.; Academic: New York, 1978; Vol. III, pp 347–393.
(33) Asher, S. A. *Methods Enzymol.* **1981**, *76*, 341–413.
(34) Spiro, T. G. In *Iron Porphyrins*; Lever, A. B. P., Gray, H. B., Eds.; Addison-Wesley: Reading, MA, 1983; Part 2, pp 85–159.
(35) Andersson, L. A.; Loehr, T. M.; Chang, C. K.; Mauk, A. G. *J. Am. Chem. Soc.* **1985**, *107*, 182–191.
(36) Fujiwara, M.; Tasumi, M. *J. Phys. Chem.* **1986**, *90*, 250–255.
(37) Fujiwara, M.; Tasumi, M. *J. Phys. Chem.* **1986**, *90*, 5646–5650.
(38) Ozaki, Y.; Iriyama, K.; Ogoshi, H.; Ochiai, T.; Kitagawa, T. *J. Phys. Chem.* **1986**, *90*, 6105–6112.
(39) Lutz, M.; Kleo, J. *Biochim. Biophys. Acta* **1979**, *546*, 365–369.
(40) Lutz, M.; Hoff, A. J.; Brêhamet, L. *Biochim. Biophys. Acta* **1982**, *679*, 331–341.
(41) Robert, B.; Lutz, M. *Biochim. Biophys. Acta* **1985**, *807*, 10–23.
(42) Abe, M.; Kitagawa, T.; Kyogoku, Y. *J. Chem. Phys.* **1978**, *69*, 4526–4534.
(43) Callahan, P. M.; Babcock, G. T. *Biochemistry* **1981**, *20*, 952–958.

studied are 1285, 1116, and 1060 cm^{-1}; these may be associated with the bending vibrations, $\delta(C_mH)$, which are insensitive to changes in core size. The empirical correlations established here allow structural conclusions to be made concerning BChl *a* ligation states; however, a more exact description of the vibrations awaits a normal coordinate calculation on BChl *a* and a more detailed compendium of model spectra.

The above correlations apply to monomeric BChl *a* RR spectra taken at or near room temperature. In a low-temperature study of BChl *a* at 77 K, all the samples that were five-coordinate oxygen and nitrogen liganded species at room temperature displayed a band A position of 1595 cm^{-1}, indicative of six-coordination at the central Mg^{2+} (data not shown). These results indicate that spectra of isolated BChl *a* taken at low *T* cannot be used to identify the room-temperature structures; i.e., the equilibrium constant for axial ligation is temperature sensitive.

Examples of monomeric BChl *a* in vivo that may be analyzed by the structural correlations presented here are: monomeric BChl *a* in the RC from *Rb. sphaeroides*[2] and monomeric B800 in the B800-850 antenna complex from *Rb. sphaeroides*[44]. The Q_y band of monomeric BChl *a* in the RC is electronically coupled to the BChl *a* "special pair" P865, and excited-state $\pi-\pi^*$ effects have not been considered here so any structural conclusions would not be valid. However, in the oxidized state of the RC, the two monomeric BChl *a* molecules have a weaker electronic interaction with P865.[45] In this form, the Q_x absorption maxima are observed at ≈590 nm[46] and the band A frequency position of all the BChl *a* pigments appears at 1610 cm^{-1}, with downshifted acetyl stretching frequencies.[47] Therefore, we conclude that the structure of monomeric RC BChl *a* is five-coordinate, with a nitrogenous ligand and hydrogen bonding involved at the ring periphery. This is consistent with the X-ray crystal structure description of these pigments.[48]

Another monomeric BChl *a* pigment can be found in the antenna protein B800-850. The Q_x band of the B800 antenna pigment was identified at 585 nm by linear dichroism studies[44] and its band A position is at 1610 cm^{-1}.[41] The RR spectra also indicate strong interactions at the acetyl group.[41] Thus, a nitrogen ligand to BChl *a* resulting in five-coordinate Mg^{2+} and a hydrogen bond at the ring periphery is again the presumed structure. This coordination conclusion is consistent with the low-frequency RR data of Robert and Lutz[41] and with the presence of a highly conserved histidine group found in the membrane spanning region of all the purple photosynthetic bacteria antenna proteins sequenced to date.[49] We are unable to speculate about mixed-ligand structures as they are difficult to prepare in solution. Futher work on absorption and RR spectroscopy of aggregated BChl *a* model systems and a more complete study of hydrogen bonding on the spectrum of BChl *a* are being carried out in order to provide structural conclusions for additional BChl *a*–protein systems.

Acknowledgment. Isolation of BChl *a* and BPheo *a* by Constance Rose and financial support from NIH Grant GM35108 are gratefully acknowledged.

Registry No. BChl *a*, 17499-98-8; BPheo *a*, 17453-58-6.

(44) Bolt, J.; Sauer, K. *Biochim. Biophys. Acta* **1979**, *546*, 54–63.
(45) Kirmaier, C.; Holten, D.; Parson, W. *Biochim. Biophys. Acta* **1985**, *810*, 49–61.
(46) Sauer, K. *Acc. Chem. Res.* **1978**, *11*, 257–264.
(47) Zhou, Q.; Robert, B.; Lutz, M. *Biochim. Biophys. Acta* **1987**, *890*, 368–376.
(48) Allen, J. P.; Feher, G.; Yeates, T. O.; Rees, R. C.; Deisenhofer, J.; Michel, H.; Huber, R. *Proc. Natl. Acad. Sci. U.S.A.* **1986**, *83*, 8589–8593.
(49) Zuber, H. *Photochem. Photobiol.* **1985**, *42*, 821–844.

An ab Initio Study of the Reaction Pathways for $OH + C_2H_4 \rightarrow HOCH_2CH_2 \rightarrow$ Products

Carlos Sosa[†] and H. Bernhard Schlegel*[‡]

Contribution from the Department of Chemistry, Wayne State University, Detroit, Michigan 48202. *Received October 20, 1986*

Abstract: The energetically favorable reaction paths for the unimolecular decomposition of the primary addition product of $OH + C_2H_4$ have been studied with ab initio techniques. Equilibrium geometries and transition structures were fully optimized with 3-21G and 6-31G* basis sets at the Hartree–Fock level. Heats of reaction and barrier heights have been computed with Møller–Plesset perturbation theory up to fourth order, with and without annihilation of spin contamination. At the MP4 level barrier heights are lowered by 2–7 kcal/mol when the largest spin contaminant is removed. After the addition of $OH + C_2H_4$ to form the 2-hydroxyethyl radical, the most favorable reaction path (other than decomposition to reactants) is the [1,3]-hydrogen shift to form ethoxy radical followed by a dissociation into $CH_3 + CH_2O$. Other slightly higher energy paths include dissociation of ethoxy into $H + CH_3CHO$ and decomposition of the 2-hydroxyethyl radical into $H + HOCHCH_2$.

The hydroxyl radical plays an important role both in combustion processes and in atmospheric chemistry.[1] To a large extent, the fate of alkenes in the atmosphere is governed by their reaction with OH. In turn, the reaction with alkenes is an important factor controlling the atmospheric concentration of OH. These reactions are dominated by electrophilic addition,[2-19] with hydrogen abstraction occurring only at higher temperatures.[1,20,21] For the simplest alkene, ethylene, OH addition produces chemically activated 2-hydroxyethyl radical **1**, which can be collisionally stabilized, or revert to reactants, or react further to yield a variety

Scheme I

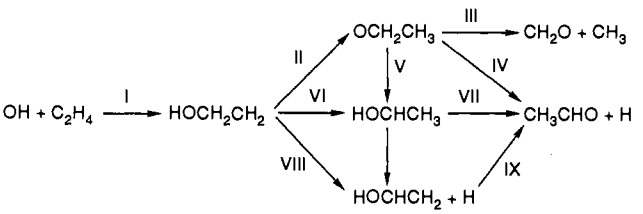

[†]Present address: Quantum Theory Project, University of Florida, Gainesville, FL 32605.
[‡]Camille and Henry Dreyfus Teacher-Scholar.

0002-7863/87/1509-7007$01.50/0